

## Adsorption characteristics of tetracycline antibiotics from aqueous solution onto graphene nanoplatelets: Equilibrium, kinetic and thermodynamic studies

Dian-Peng Sui<sup>a,\*</sup>, Hong-Hong Li<sup>a</sup>, Yuan Chai<sup>a</sup>, Jian Li<sup>b</sup>, Shuang Liu<sup>b</sup>, Yue Zhao<sup>c</sup>, Hong-Tao Fan<sup>b,\*</sup>, Hong-Bo Xu<sup>c,\*</sup>

<sup>a</sup>College of Sciences, Northeastern University, Shenyang 110004, China, email: sdp2596@163.com (D.-P. Sui), 841327379@qq.com (H.-H. Li), ChaiYuan0901@163.com (Y. Chai)

<sup>b</sup>College of Applied Chemistry, Shenyang University of Chemical Technology, Shenyang, 100142, Liaoning, China, 775656387@qq.com (J. Li), liushuang295726820@foxmail.com (S. Liu), httyf\_77@163.com (H.-T. Fan)

<sup>c</sup>College of Chemical Technology, University of Science and Technology Liaoning, Anshan, 114051, email: 284641819@qq.com (Y. Zhao), Tel. 86-24-89383297, email: anshanxuhb@163.com (H.-B. Xu)

Received 18 January 2017; Accepted 30 October 2017

### ABSTRACT

A systematic study of the adsorption characteristics of commercial graphene nanoplatelets for tetracycline antibiotics (such as tetracycline, oxytetracycline, and chlortetracycline) was performed by varying pH, ionic strengths, contact time, temperature, and initial concentrations. Meanwhile, isothermal, kinetic and thermodynamic constants were also determined. The experimental results indicated that graphene is a potential effective adsorbent for tetracycline antibiotics with high adsorption capacity of up to 207.2 mg g<sup>-1</sup> for tetracycline, 240.4 mg g<sup>-1</sup> for chlortetracycline and 232.7 mg g<sup>-1</sup> for oxytetracycline from aqueous solutions. The solution pH in the range of 4–8 had a minor effect on the adsorption of three antibiotics. The adsorption kinetics of three antibiotics was found that the equilibrium was reached within 30 min following the pseudo-second-order model with high correlation coefficients (>0.99). The adsorption data could be well fitted by the Langmuir model. Moreover, the calculation of thermodynamic parameters indicated that the adsorption process of three antibiotics onto graphene nanoplatelets was the endothermic and spontaneous nature.

*Keywords:* Graphene; Tetracycline; Oxytetracycline; Chlortetracycline; Adsorption

### 1. Introduction

The tetracyclines (TCs) family, such as tetracycline (TC), oxytetracycline (OTC), and chlortetracycline (CTC), is broad spectrum antibiotics for their good activity against acute diseases caused by gram-positive and gram-negative bacteria [1], and has been widely applied in livestock and poultry farming industry as therapeutic agents for infectious diseases or as growth promoters for controlling bacterial infections and improving feed efficiency [2]. Only small portions of TCs ingested are metabolized or absorbed *in vivo*, and most of TCs is eliminated as metabolite forms through urine or feces of animals into the environment [3,4].

TCs have been a class of potential environmental pollutants due to the development of microorganism resistance in the nature and serious threats to environment and human health [5,6]. TCs contaminated water should be treated properly to meet the regulations. Therefore, the efficient methods for removal of TCs from aqueous solution have attracted considerable attention in recent years.

At present, treatment technologies (such as advanced oxidation processes [7], radiolysis [7], membrane separation [8], bioadsorption [9], adsorption [9], electrochemical processes [10] and photocatalysis degradation [11]) have been used for the removal of TCs from aqueous solution. Among these methods, adsorption is considered to be a simple, economical, efficient and practical method for TCs

\*Corresponding author.

removal from wastewater even at low concentration as well as the availability of a wide range of adsorbents. Till now, various sorbents (such as activated carbon [9], resin [12], metal oxide [13], cellulose [14], minerals [15], modified silica [16], biomass [17], carbon nanotubes [18], zero valent iron [19], graphene-like MoS<sub>2</sub> [20] and graphene-like BN [21]) have been utilized to remove TCs from aqueous solution. However, a challenging issue of adsorption is lack of the high efficient sorbents.

In recent years, graphene, a novel two-dimensional carbonaceous nanomaterial composed of sp<sup>2</sup>-hybridized graphitic carbon [22,23], attracts a tremendous attention as a superior sorbents for the removal of pollutants [24–32]. This importance is greatly attributed to its unique conjugated structure, which exhibits high adsorption capacity for various organic pollutants through  $\pi$ - $\pi$  stacking interactions or/and cation- $\pi$  bonding [33–36]. TCs antibiotics consist of four aromatic rings with various functional groups on each ring [1]. Recently, Ghadim et al. [35] and Gao et al. [36] reported graphene oxide as effective adsorbent for TCs which strongly deposited on the surface of graphene oxide via  $\pi$ - $\pi$  interactions and cation- $\pi$  bonding. However, until now, it can be noticed that no detailed study are available on using commercial graphene nanoplatelets as an adsorbent in removing TCs from aqueous solution and not much investigation has been carried on the adsorption characteristics, isotherm, kinetic and thermodynamic of TCs onto commercial graphene nanoplatelets.

In the present work, commercial graphene nanoplatelets were used as the sorbent to remove three representative TCs antibiotics, including TC, OTC and CTC. The influencing factors, such as solution pH, ionic strengths, initial concentration, contact time and temperature, had been investigated to obtain the optimal conditions for the adsorption of TCs from aqueous solutions. The kinetic, isothermal and thermodynamic analyses were also assessed.

## 2. Experimental

### 2.1. Chemicals and solution

TC, OTC and CTC were of HPLC-grade and purchased from Aladdin (Shanghai, China). Graphene nanoplatelets aggregates (sub-micronparticles, S.A 500 m<sup>2</sup> g<sup>-1</sup>) were purchased from Alfa Aesar. All the other reagents used in this work were analytically pure. The stock solutions of TC, OTC and CTC (1000 mg L<sup>-1</sup>) was prepared by dissolving the required amount of TCs in distilled water. Work solutions of TCs were prepared by the series dilution of the stock solutions.

### 2.2. Characterization

The FT-IR spectra of the virgin and TCs-loaded graphene nanoplatelets were recorded on NICOLET 6700 (Thermal scientific Inc. USA) instrument with the range of 4000–400 cm<sup>-1</sup> in KBr medium at room temperature. Morphological studies were accomplished through scanning electronic microscopy (SEM) coupled with energy dispersive X-ray (EDX) spectroscopy, using a Hitachi SU8000 microscope.

### 2.3. Adsorption experiments

Adsorption experiments were implemented by a batch equilibration mode, which added 100 mg (OHAUS analytical balance, model FR124CN, the nearest of 0.0001 g) of graphene nanoplatelets into 25.00 mL TCs solution of known concentration with stirring at 200 rpm, allowed to equilibrate at the desired equilibrium time and desired temperature, and analyzed subsequently the residual concentrations of TCs in supernatant solution by centrifuging for 10 min at 4000 rpm after equilibrium. Adsorption studies were performed at various time intervals (10, 20, 30, 40, 50 and 60 min), at different initial concentrations of TCs (100, 200, 300, 400, 500, 600, 700, 800, 900 and 1000 mg L<sup>-1</sup>), at various solution pH (2, 3, 4, 5, 6, 7, 8, 9, 10 and 11), at different ionic strengths (0.0001, 0.0005, 0.001, 0.005, 0.01, 0.05, 0.1, 0.5 and 1 mol L<sup>-1</sup>) and at various temperature (20, 30, 40 and 50°C). The pH was adapted by the solutions of HCl (0.1 mol L<sup>-1</sup>) or NaOH (0.1 mol L<sup>-1</sup>). The measurement of pH was carried out using a pH meter (ST20, OHAUS). After equilibrium, the residual concentrations of TCs were determined by a colorimetric method. The adsorption capacities or amounts of TCs onto graphene nanoplatelets ( $q_e$ , mg g<sup>-1</sup>) were calculated by the following formula:

$$q_e = (C_i - C_e) \cdot V/m \quad (1)$$

where  $C_i$  is the initial concentration of TCs (mg L<sup>-1</sup>);  $C_e$  is the equilibrium or residual concentrations of TCs (mg L<sup>-1</sup>);  $V$  is the volume of the feed solution (L); and  $m$  is the mass of sorbent (g). The experiments were performed in three replicates. The standard statistical methods were used to determine the mean values and standard deviations. The margin of error was calculated by using confidence intervals of 95 % for each set of data.

### 2.4. Analytical determination of TCs contents

The residual concentrations of TCs were determined by a colorimetric method [37,38]. The analytical determinations of TCs were carried out using UV-VIS spectrophotometer (Shimadzu, Model UV-2550) by analyzing colour resulting from the complexation of the TCs with cupric chloride in alkaline medium [37,38]. The maximum absorption wavelengths of yellowish green copper complexes of TC, OTC and CTC against a reagent blank were found to be at 400, 395 and 410 nm, respectively [37,38]. The calibration curves of TCs at maximum absorption wavelength were established as a function of TCs concentrations. The linear calibration curves were gained in the range from 0.5 to 10 mg L<sup>-1</sup> for TCs. The reproducibility of the data varied in the range of  $\pm 2\%$ .

## 3. Results and discussion

### 3.1. Effects of pH

It has been established that the pH of solution is an important parameter in the adsorption process, which affects the chemical speciation of the adsorbates, the activity of the functional groups on the adsorbents and the

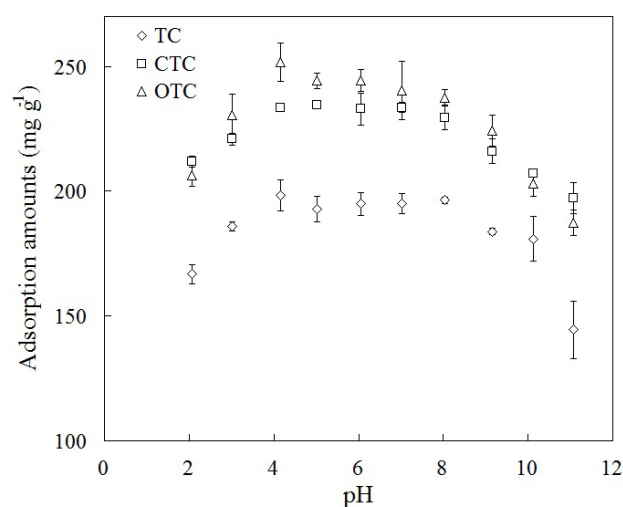


Fig. 1. Effects of pH on the adsorption amounts of graphene nanoplatelets for TCs: Concentration of TCs = 600 mg L<sup>-1</sup>, time = 30 min, temperature = 20°C.

removal efficiency of the adsorbates [39]. Fig. 1 shows the pH dependence of TCs adsorption onto the graphene nanoplatelets. The adsorption amounts of the TCs on the graphene nanoplatelets increased with the increase of pH up to 4. The stable adsorption amounts of TCs were found to occur in the range of pH 4–8. When pH > 8, the low adsorption amounts of TCs were observed. The pH dependent phenomenon might be related to not only a change in chemical speciation of TCs compounds, but also the protonation–deprotonation transition of graphene nanoplatelets. The TCs molecular conformations can exist as cation at pH < 4, the neutral form at pH between 4 and 8, and anion at pH > 8 [40]. At pH below 4, the surface of graphene nanoplatelets was protonated. The electrostatic repulsion between the positive charges of graphene nanoplatelets surface and the cationic species of the TCs resulted in the low adsorption amounts. Under moderately acidic, neutral and weak alkaline conditions (pH 4–8), the high stable adsorption amounts of the TCs were obtained through  $\pi$ - $\pi$  interactions and cation- $\pi$  bonding [36]. At pH > 8, the  $\pi$ - $\pi$  interactions and cation- $\pi$  bondings between the TCs and graphene were suppressed with increase of pH due to the weakening of electron-acceptor ability of the TCs. Hence, pH of 5 was chosen in subsequent works.

### 3.2. Effects of ionic strength

Effects of ionic strengths of feed solution on the adsorption amounts of graphene nanoplatelets for TCs are given in Fig. 2. In the entire experimental range of ionic strengths from 0.0001 to 1 mol L<sup>-1</sup> (as NaCl), the adsorption amounts of TCs on the graphene nanoplatelets remained almost constant. The results indicated that the adsorption of TCs was not significantly affected by electronic screening interactions [36,41], whereas was mainly due to  $\pi$ - $\pi$  dispersive interactions [42]. The same trends were also observed by Zhang et al. [18] and Carrales-Alvarado et al. [42] which used various carbon materials as sorbents.

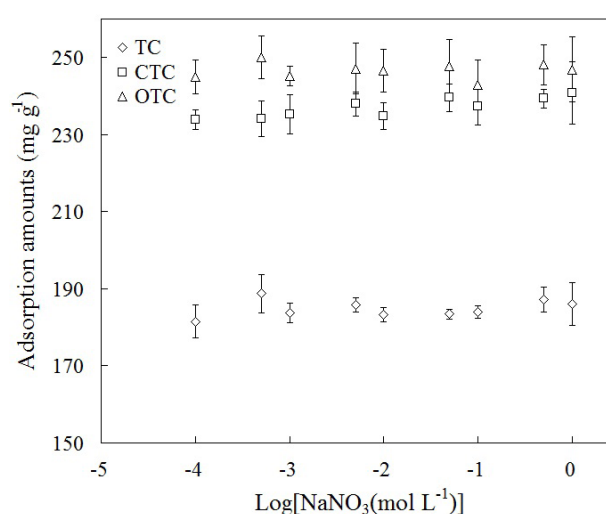


Fig. 2. Effects of ionic strengths on the adsorption amounts of graphene nanoplatelets for TCs: Concentration of TCs = 600 mg L<sup>-1</sup>, time = 30 min, pH = 5, temperature = 20°C.

### 3.3. Effects of contact time

The adsorption rate is of most important when designing batch adsorption experiments. The dependence between the contact time and the adsorption amounts of TCs on graphene nanoplatelets is shown in Fig. 3. As seen here, the adsorption amounts of TCs increase with the contact time during the first 30 min, which could be attributed to the number and availability of active sites on the surface of graphene nanoplatelets, as well as the highest driving force for the mass transfer resulting in the rapid uptake of TCs at the beginning, and equilibrium seems to achieve after 30 min due to the saturation of the available active sites on the surface of graphene nanoplatelets. Therefore, an equilibrium time of 30 min was adopted for all subsequent batch studies.

### 3.4. Effects of the initial concentrations

The effects of TCs concentrations on the adsorption amounts of TCs on the graphene nanoplatelets are shown in Fig. 4. It could be seen that the adsorption amounts of TCs increased with increasing the initial concentrations of TCs in the range of 100–500 mg L<sup>-1</sup> due to the increase in the driving force of concentration gradient with the increase of the initial concentrations of TCs, and showed a little variation in the range of the initial concentrations of TCs from 600 to 1000 mg L<sup>-1</sup> which was probably due to the saturation of the active sites on the adsorbent surface with the increase of the concentrations of TCs. The experimental values of maximum adsorption capacities of graphene nanoplatelets for TC, CTC and OTC were found to be 207.2, 240.4 and 232.7 mg g<sup>-1</sup>, respectively.

Table 1 compares the adsorption capacities of TCs by different adsorbents reported in the literature [9,12–18,36,40]. It was found that the graphene nanoplatelets gave a relatively high adsorption capacity than most adsorbents reported in the literature. Compared with the other adsorbents, carbon-based adsorbents own higher adsorption capacities for

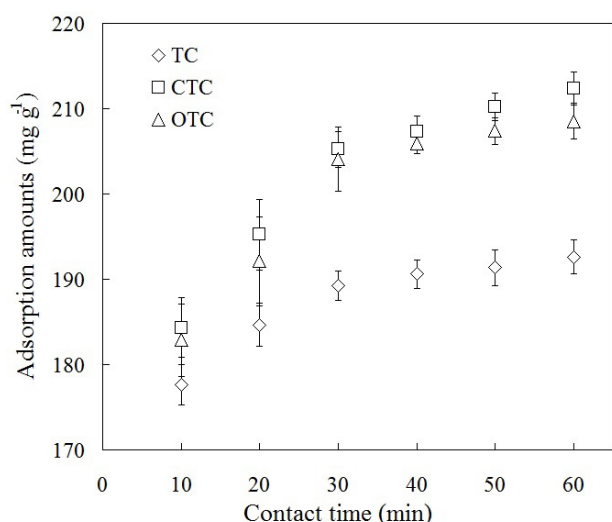


Fig. 3. Effects of contact time on the adsorption equilibrium of TCs onto graphene nanoplatelets: Concentration of TCs = 600 mg L<sup>-1</sup>, pH = 5, temperature = 20°C.

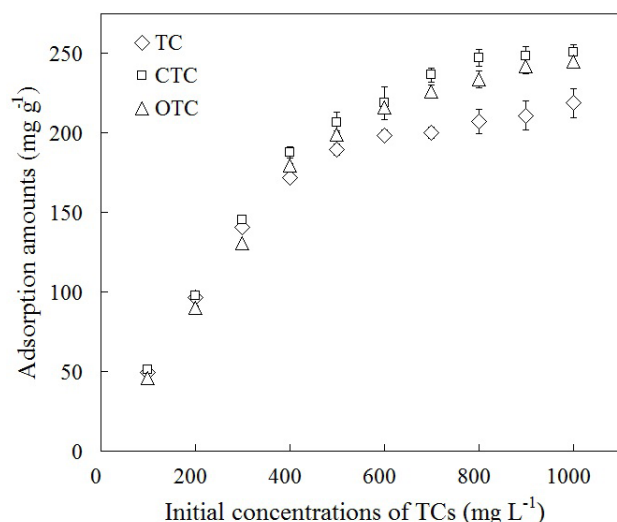


Fig. 4. Effects of initial concentrations of TCs on the adsorption amounts of graphene nanoplatelets for TCs: pH = 5, time = 30 min, temperature = 20°C.

TCs due to the different adsorption mechanisms between TCs and adsorbents, indicating that the interaction between the functional groups of adsorbents and TCs is believed to be one of the factors contributing to the different adsorption characteristics [17]. The slight difference of adsorption capacity by carbon-based adsorbent for TCs may due to different investigated conditions.

### 3.5. Adsorption kinetics

Since the adsorption amount of an adsorbent depends upon the contact time, the study of the kinetics of adsorption is a vital factor. The adsorption is governed by the arrival rate of TCs to the surface of the adsorbent and the propor-

tion of the incident TCs which gets adsorbed. Three of the most widely used kinetic models, that is, pseudo-first-order, pseudo-second-order and intraparticle diffusion equations, were considered to interpret the time dependent experimental data. The linear expression of pseudo-first-order rate equation is [43]

$$\log (q_e - q_t) = \log q_e - k_1 t / 2.303 \quad (2)$$

where  $k_1$  (min<sup>-1</sup>) is the rate constant of the pseudo-first-order adsorption.  $q_e$  and  $q_t$  (mg g<sup>-1</sup>) are the adsorption amounts at equilibrium and at time  $t$  (min), respectively. The rate constants  $k_1$ ,  $q_e$  and correlation coefficients  $r^2$  were calculated using the slope and intercept of plots of  $\log (q_e - q_t)$  versus  $t$ .

The linear expression of pseudo-second-order rate equation is described as: [44]

$$t/q_t = 1/k_2 q_e^2 + t/q_e \quad (3)$$

where  $k_2$  (g mg<sup>-1</sup> min<sup>-1</sup>) is the rate constant of the pseudo-second-order model. The linear constructions of  $t/q_t$  vs.  $t$  were charted. The slopes and intercepts of these curves were used to obtain the values of  $k_2$ ,  $q_e$  and correlation coefficients  $r^2$ .

The intraparticle diffusion model is linearly expressed as [45]

$$q_t = k_{pi} t^{0.5} + C_{pi} \quad (4)$$

where  $k_{pi}$  is the intraparticle diffusion rate constant of stage  $i$  (mg g<sup>-1</sup> min<sup>-0.5</sup>), and is calculated by the slope of straight-line portion of plotting  $q_t$  vs  $t^{0.5}$ .  $C_{pi}$ , the intercept of stage  $i$ , gives an idea about the thickness of boundary layer [46].

It was found that the  $r^2$  values of TCs for the pseudo-first-order model (0.8924 for TC, 0.9257 for CTC and 0.8674 for OTC) were lower than the pseudo-second-order equation (0.9999 for TC, 0.9999 for CTC and 0.9998 for OTC) (as presented in Table1). This implied that the adsorption did not comply with pseudo-first-order equation. It was clear from Table 2 that the calculated value of adsorption capacities of TCs onto the graphene nanoplatelets (196.1 mg g<sup>-1</sup> for TC, 217.4 mg g<sup>-1</sup> for CTC and 217.4 mg g<sup>-1</sup> for OTC) at equilibrium from the slope of the pseudo-second-order plot were in good agreement with the experimental values of adsorption capacities of TCs (207.2 mg g<sup>-1</sup> for TC, 240.4 mg g<sup>-1</sup> for CTC and 232.7 mg g<sup>-1</sup> for OTC). Compared with pseudo-first-order model, the results indicated that the pseudo-second-order model was able to satisfactorily fit the kinetic data for the adsorption of TCs onto the graphene nanoplatelets in the whole data range. The consistency of the experimental data with the pseudo-second-order kinetic model indicated that the adsorption of TCs on the graphene was controlled by chemical adsorption (chemisorption) involving the  $\pi$ - $\pi$  interactions and cation- $\pi$  bondings between adsorbent and adsorbate.

The pseudo-first-order and pseudo-second-order equations could not distinguish the diffusion mechanism. The data were then examined by the intraparticle diffusion model. According to the model, the curve of  $q_t$  vs.  $t^{1/2}$  can be linear if intraparticle diffusion is related to the adsorp-

Table 1  
Comparison of the adsorption capacities of various sorbents toward TCs from the literatures

Adsorbents	Capacities of TCs (mg g <sup>-1</sup> )			Ref.
	TC	OTC	CTC	
Activated carbon	375.4	252.6	65.1	[9]
Resin	117.3	–	–	[12]
Metal oxide	28.4	–	–	[13]
Cellulose	8.0	–	–	[14]
Hydroxyapatite/ clay composites	76.0	–	–	[15]
Hydroxyapatite/ pumice composites	179	–	–	[15]
Modified silica	112.3	–	–	[16]
<i>S. Hemiphyllum</i>	4.0	–	–	[17]
<i>P. Coriaceum</i>	9.0	–	–	[17]
Carbon nanotubes	269.5	–	–	[18]
Graphene oxide	313.5	212.3	–	[36]
Montmorillonite	250	–	–	[40]
Graphene nanoplatelets	207.2	240.4	232.7	This work

tion. If the plots go through the origin then intraparticle diffusion is the rate-determining step [47]. As can be seen in Table 1, the data points are related by two straight lines. The first sharper portion was attributed to the diffusion of adsorbate through the solution to the external surface of the adsorbent (external diffusion) and the second portion described the gradual adsorption stage, corresponding to diffusion of adsorbate molecules inside the pores of the adsorbent (intraparticle diffusion) [46]. The large values of the intercept indicated the remarkable boundary layer effect [48]. The curves did not go through the origin. This might be indicative of some degree of boundary layer control. This also implies that the intraparticle diffusion does not only contribute to the rate determining step, but also other process may control the rate of adsorption simultaneously [49].

### 3.6. Adsorption isotherms

Adsorption isotherm describes the relationship between the amount of a solute adsorbed and its concentration in the equilibrium solution at a constant temperature. Adsorption isotherm is important to understand the adsorbate–adsorbent interactions and optimization of the use of adsorbents. The data were examined using the Langmuir, Freundlich and Dubinin–Radushkevich (D–R) models in order to obtain the best suitable isotherm.

The linear expression of Langmuir isotherm can be represented as the Eq. (5) [50]:

$$C_e/q_e = 1/(q_{\max} b) + C_e/q_{\max} \quad (5)$$

The linear equation of Freundlich isotherm can be described by Eq. (6) [51]:

$$\log q_e = \log k_F + (1/n) \log C_e \quad (6)$$

The linear form of D–R isotherm can be represented as [52]

$$\ln q_e = \ln q_s - k_{\text{ad}} \varepsilon^2 \quad (7)$$

where  $q_e$  is the amount of solutes adsorbed in the sorbent (mg g<sup>-1</sup>),  $C_e$  is the equilibrium concentration of solutes in solution (mg L<sup>-1</sup>),  $b$  (mL mg<sup>-1</sup>) is the equilibrium constant related to the adsorption energy, and  $q_{\max}$  is the maximum adsorption capacity (mg g<sup>-1</sup>),  $k_F$  and  $n$  are the Freundlich constants,  $k_{\text{ad}}$  is the D–R isotherm constant (mol<sup>2</sup> kJ<sup>-2</sup>)  $q_s$  is the theoretical isotherm saturation capacity (mg g<sup>-1</sup>);  $\varepsilon$  is the Polanyi potential and calculated as follows:

$$\varepsilon = RT \ln (1 + 1/C_{\text{eq}}) \quad (8)$$

where  $R$  is universal gas constant (8.314 J mol<sup>-1</sup> K<sup>-1</sup>);  $T$  is the absolute temperature (K).  $C_{\text{eq}}$  is the concentration of solutes in equilibrium solution (mol L<sup>-1</sup>).

$E$  (kJ/mol) is defined as the free energy change required transferring 1 mol of ions from solution to the solid surfaces and the magnitude of  $E$  is useful for estimating the type of adsorption reaction [53], and it is calculated from D–R parameter  $k_{\text{ad}}$  as follows:

$$E = -(2k_{\text{ad}})^{-1/2} \quad (9)$$

The plots of  $C_e/q_e$  versus  $C_e$  (Langmuir) for the adsorption of TCs onto the graphene nanoplatelets give a straight line of slope  $1/q_{\max}$  and intercept  $1/(q_{\max} b)$ ; by plotting  $\ln C_e$  versus  $\ln q_e$  (Freundlich) to generate  $k_F$  and  $n$  from the intercept and the slope, respectively; and by plotting  $\ln q_e$  versus  $\varepsilon^2$  (D–R) to obtain the value of  $q_s$  from the intercept, and the value of  $k_{\text{ad}}$  from the slope. Table 2 shows the constants of the Langmuir, Freundlich and D–R isotherms.

It can be observed from Table 3 that Langmuir isotherm model is then found to be the best-fitting isotherm compared to Freundlich and D–R isotherm models for the adsorption of TCs onto the graphene nanoplatelets. The high determination coefficient values ( $R^2 > 0.99$ ) were obtained for the Langmuir model indicating a good agreement between the experimental parameters and confirming the monolayer adsorption of TCs onto the surface of graphene nanoplatelets. The Langmuir constant  $q_{\max}$ , which were calculated from the monolayer adsorption capacity of the graphene nanoplatelets for TC, CTC and OTC, were obtained as 217.4, 256.4 and 256.4 mg g<sup>-1</sup>, respectively.

The magnitude of  $E$  is useful for estimating the type of adsorption process. The typical range of bonding energy for chemical mechanisms is  $>8$  kJ mol<sup>-1</sup> [54]. The values of  $E$  for TC, CTC and OTC at 298.15 K obtained from D–R isotherms were 15.81, 15.43 and 12.31 kJ mol<sup>-1</sup>, respectively, which were more than the energy range of chemical adsorption reaction, indicating that chemisorption mechanism may play a significant role in the adsorption process of TCs onto graphene nanoplatelets [54]. The graphene nanoplatelets offered electron donor and a homogenous surface for the adsorption of TCs, which led to better fitting of TCs adsorption on the surface of graphene nanoplatelets to Langmuir model.

Table 2  
Calculated kinetic parameters for the adsorption of TCs onto the graphene nanoplatelets

Adsorbates	Pseudo-first-order model	Pseudo-second-order model	Intraparticle diffusion model
TC	$k_1 = 0.0134 \text{ min}^{-1}$	$k_2 = 4.56 \times 10^{-3} \text{ g} \cdot \text{mg}^{-1} \cdot \text{min}^{-1}$	$k_{p1} = 5.034 \text{ mg} \cdot \text{g}^{-1} \cdot \text{min}^{-1}$ $r^2 = 0.9976$
	$q_{\text{eq}}(\text{cal}) = 30.2 \text{ mg} \cdot \text{g}^{-1}$ $r^2 = 0.8924$	$q_{\text{eq}}(\text{cal}) = 196.1 \text{ mg} \cdot \text{g}^{-1}$ $r^2 = 0.9999$	$k_{p2} = 1.444 \text{ mg} \cdot \text{g}^{-1} \cdot \text{min}^{-1}$ $r^2 = 0.9892$
	$k_1 = 0.0136 \text{ min}^{-1}$	$k_2 = 2.14 \times 10^{-3} \text{ g} \cdot \text{mg}^{-1} \cdot \text{min}^{-1}$	$k_{p1} = 8.989 \text{ mg} \cdot \text{g}^{-1} \cdot \text{min}^{-1}$ $r^2 = 0.9974$
CTC	$q_{\text{eq}}(\text{cal}) = 59.1 \text{ mg} \cdot \text{g}^{-1}$ $r^2 = 0.9257$	$q_{\text{eq}}(\text{cal}) = 217.4 \text{ mg} \cdot \text{g}^{-1}$ $r^2 = 0.9999$	$k_{p2} = 3.1965 \text{ mg} \cdot \text{g}^{-1} \cdot \text{min}^{-1}$ $r^2 = 0.9930$
	$k_1 = 0.0145 \text{ min}^{-1}$	$k_2 = 2.33 \times 10^{-3} \text{ g} \cdot \text{mg}^{-1} \cdot \text{min}^{-1}$	$k_{p1} = 9.075 \text{ mg} \cdot \text{g}^{-1} \cdot \text{min}^{-1}$ $r^2 = 0.9775$
OTC	$q_{\text{eq}}(\text{cal}) = 52.5 \text{ mg} \cdot \text{g}^{-1}$ $r^2 = 0.8674$	$q_{\text{eq}}(\text{cal}) = 217.4 \text{ mg} \cdot \text{g}^{-1}$ $r^2 = 0.9998$	$k_{p2} = 1.951 \text{ mg} \cdot \text{g}^{-1} \cdot \text{min}^{-1}$ $r^2 = 0.9976$

### 3.7. Thermodynamic study

To assess the spontaneity of adsorption, energy and entropy should be considered. Values of thermodynamic parameters such as standards Gibbs free energy change ( $\Delta G^\circ$ ) enthalpy change ( $\Delta H^\circ$ ) and entropy change ( $\Delta S^\circ$ ) are the actual indicators for practical application of a process. The amounts adsorbed of TCs at different temperatures (293.15, 303.15, 313.15 and 323.15 K) have been examined to obtain thermodynamic parameters for the adsorption system. The thermodynamic parameters can be gained according to the following equations:

$$\Delta G^\circ = -RT \ln K_0 \quad (10)$$

$$\ln K_0 = \frac{\Delta S^\circ}{R} - \frac{\Delta H^\circ}{RT} \quad (11)$$

where  $T$  is the solution temperature (K) and  $R$ , the gas constant.  $K_0$  can be defined as [55]:

$$K_0 = \frac{a_s}{a_e} = \frac{\gamma_s C_s}{\gamma_e C_e} \quad (12)$$

where  $a_s$  is the activity of adsorbed adsorbates,  $a_e$  is the activity of adsorbates in solution at equilibrium,  $\gamma_s$  is the activity coefficient of adsorbed adsorbates,  $\gamma_e$  is the activity coefficient of adsorbates in equilibrium solution,  $C_s$  is the adsorbates adsorbed on sorbent ( $\text{mmol g}^{-1}$ ), and  $C_e$  is the concentration of adsorbates in equilibrium solution ( $\text{mol L}^{-1}$ ).  $K_0$  can be compressed by supposing  $C_s \rightarrow 0$  and  $C_e \rightarrow 0$  and the activity coefficients are close to 1 [55]. Eq. (12) can be written as:

$$C_s \xrightarrow{\text{lim}} 0 \frac{C_s}{C_e} = \frac{a_s}{a_e} = K_0 \quad (13)$$

$K_0$  can be gained by plotting  $\ln(C_s/C_e)$  vs.  $C_s$  and extrapolation  $C_s$  to zero [55].  $\Delta H^\circ$  and  $\Delta S^\circ$  were obtained from the slope and intercept of Eq. (11).

The all negative values  $\Delta G^\circ$  demonstrate the thermodynamically practicable and spontaneous nature of adsorp-

Table 3  
Isotherms parameters for the adsorption of TCs onto the graphene nanoplatelets

Adsorbates	Langmuir isotherm	Freundlich isotherm	Dubinin–Radushkevich isotherm
TC	$q_{\text{max}} = 217.4 \text{ mg} \cdot \text{g}^{-1}$ $b = 0.0721 \text{ L} \cdot \text{mg}^{-1}$ $R^2 = 0.9984$	$k_F = 56.4$ $n = 4.31$ $R^2 = 0.8957$	$k_{\text{ad}} = 0.002 \text{ mol}^2 \cdot \text{kJ}^{-2}$ $q_s = 420.6 \text{ mg} \cdot \text{g}^{-1}$ $E = 15.721 \text{ kJ} \cdot \text{mol}^{-1}$ $R^2 = 0.9386$
	CTC	$q_{\text{max}} = 256.4 \text{ mg} \cdot \text{g}^{-1}$ $b = 0.1057 \text{ L} \cdot \text{mg}^{-1}$ $R^2 = 0.9993$	$k_F = 71.2$ $n = 4.37$ $R^2 = 0.7649$
OTC		$q_{\text{max}} = 256.4 \text{ mg} \cdot \text{g}^{-1}$ $b = 0.0302 \text{ mL} \cdot \text{g}^{-1}$ $R^2 = 0.9995$	$k_F = 31.7$ $n = 2.82$ $R^2 = 0.9068$

tion (in Table 4). Also, the existence of more negative  $\Delta G^\circ$  at higher temperatures suggested that the inclination toward the spontaneous nature of reaction was more at higher temperatures. The positive values of the enthalpy change ( $21.7 \text{ kJ mol}^{-1}$  for TC,  $11.4 \text{ kJ mol}^{-1}$  for CTC and  $17.2 \text{ kJ mol}^{-1}$  for OTC) indicated that the adsorption was chemical in nature involving strong forces of attraction and was also endothermic [54]. The positive values ( $96.6 \text{ J mol}^{-1} \text{ K}^{-1}$  for TC,  $64.5 \text{ J mol}^{-1} \text{ K}^{-1}$  for CTC and  $82.2 \text{ J mol}^{-1} \text{ K}^{-1}$  for OTC) of entropy change ( $\Delta S^\circ$ ) corresponded to an increase in the degree of randomness at the adsorbents and adsorbates interface in the course of adsorption of TCs onto the graphene nanoplatelets, which could be attributable to a remarkable desolvation of the molecules of solute passing from the solution to the surface of the adsorbents [56,57]. Based on those thermodynamics constants, the adsorption of TCs onto the graphene nanoplatelets gave a spontaneous and endothermic process.

Table 4  
Various thermodynamic constants for the adsorption of TCs onto the graphene nanoplatelets

Adsorbates	Temperature (K)	Thermodynamic constants			
		$K_0$	$\Delta G^\circ$ (kJ mol <sup>-1</sup> )	$\Delta H^\circ$ (kJ mol <sup>-1</sup> )	$\Delta S^\circ$ (J mol <sup>-1</sup> K <sup>-1</sup> )
TC	293.15	15.54	-6.69		
	303.15	19.43	-7.48	21.7	96.6
	313.15	24.77	-8.36		
	323.15	36.07	-9.63		
CTC	293.15	21.63	-7.49		
	303.15	25.34	-8.15	11.4	64.5
	313.15	29.97	-8.85		
	323.15	33.11	-9.40		
OTC	293.15	16.97	-6.90		
	303.15	21.63	-7.75	17.2	82.2
	313.15	27.49	-8.63		
	323.15	32.37	-9.34		

### 3.8. Analysis of graphene nanoplatelets before and after TC adsorption

The mechanism for strong adsorption of TC on graphene is not clear yet [36].  $\pi$ - $\pi$  stacking interaction as a dominant driving force has always been used to explain the mechanism of aromatic adsorbate to graphene surface [36]. The adsorption mechanism of graphene nanoplatelets for TC was explored by the FT-IR spectrum and SEM-EDS. FT-IR spectra of the virgin graphene nanoplatelets and the TC-loaded samples are depicted in Fig. 5. Graphene has two characteristic FT-IR peaks at 1650 cm<sup>-1</sup> which is attributed to the C=C stretching vibration and at 1112 cm<sup>-1</sup> due to C-C skeletal vibration of graphene [58]. The peak at 3450 cm<sup>-1</sup> and 1467 cm<sup>-1</sup> are assigned to the O-H stretching and deformation vibrations due to adsorbed water. For the TC-loaded graphene nanoplatelets, the peaks at 3450 cm<sup>-1</sup> and 1459 cm<sup>-1</sup> are assigned to the O-H stretching and deformation vibrations of hydroxyl groups. The peaks at 3289 and 1388 cm<sup>-1</sup> are due to the N-H stretching and bending vibrations. Both symmetric and asymmetric C-H stretching vibrations are observed at 2857–2968 cm<sup>-1</sup> for the TC-loaded graphene nanoplatelets. The peak at 1120 cm<sup>-1</sup> is attributed to the C-N stretching vibration. These peaks prove the existence of TC. After TC adsorption onto graphene nanoplatelets, the vibration of C=C skeleton shifted about 30 cm<sup>-1</sup> higher, suggesting that the  $\pi$ - $\pi$  stacking interactions between the rings of TC and the hexagonal cells of graphene nanoplatelets probably dominate the adsorption of TC on graphene nanoplatelets [36,59].

The SEM images of the virgin and TCs-loaded graphene nanoplatelets are shown in Fig. 6. The virgin graphene nanoplatelets have a flaky sheet structure in shape with width of 10  $\mu$ m or less (Fig. 6a). Compared with the virgin graphene nanoplatelets (Fig. 6a), the general morphology of TCs-loaded graphene nanoplatelets is not greatly changed (Fig. 6b). The presence of O, N and Cl in TCs-loaded graphene nanoplatelets is clearly evident by EDX measurements (Table 5). The EDS analysis provided clear evidence

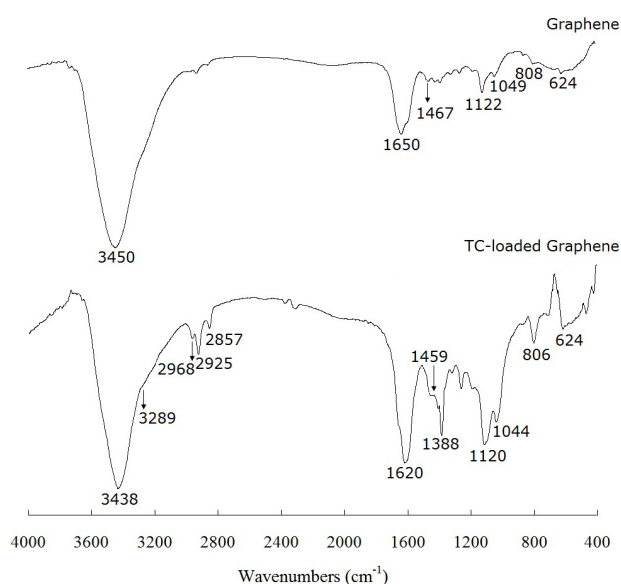


Fig. 5. IR spectrums of virgin and TC-loaded graphene nanoplatelets.

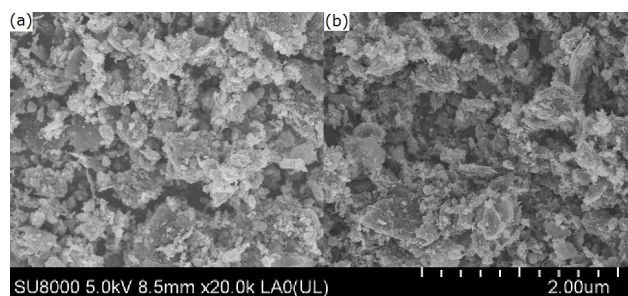


Fig. 6. SEM images of virgin (a) and TC-loaded (b) graphene nanoplatelets.

Table 5  
Contents of elements in the virgin and TC-loaded graphene nanoplatelets by EDS

Graphene nanoplatelets	Contents of elements (wt%)			
	Carbon	Oxygen	Nitrogen	Chlorinum
Virgin	99.93	0.07	N.D. <sup>a</sup>	N.D.
TC-loaded	83.85	10.62	5.53	N.D.

Note: <sup>a</sup> N.D. means not detected.

of the existence of TCs on the surface of graphene nanoplatelets, which was consistent with FT-IR analysis.

## 4. Conclusions

The kinetic studies indicated that equilibrium in the adsorption of TCs onto the graphene nanoplatelets was reached in 30 min of contact time. The optimal pH range was found to be 4–8. The ionic strengths range from 0.0001 to 1

mol L<sup>-1</sup> were independent of the amounts adsorbed of TCs on the graphene nanoplatelets. Equilibrium data analysis showed that the TCs adsorption was a monolayer adsorption on homogeneous surface. Kinetic data analysis indicated that chemical adsorption, diffusion through a boundary, or both mechanisms could be the limiting steps that controlled the adsorption process. The negative values of  $\Delta G^\circ$  and positive values of  $\Delta H^\circ$  demonstrated the spontaneous and endothermic nature. Further, the positive values of  $\Delta S^\circ$  reflected the random nature of the process at the solid–solution interface and the affinity of graphene nanoplatelets for the adsorption of TCs. Due to four aromatic rings in the molecular structure of TCs, we suggested that  $\pi$ – $\pi$  interactions probably dominate the adsorption of TCs on graphene nanoplatelets. The graphene nanoplatelets may be used as an effective material to eliminate TCs from aqueous solutions.

### Acknowledgements

The project was sponsored by the National Natural Science Foundation of China (grant no. 21477082 and 21547015), and by Liaoning Natural Science Foundation Combined with Open Foundation of Shenyang National Laboratory for Materials Sciences (grant no. 2015021019).

### References

- [1] A.A. Borghi, M.S.A. Palma, Tetracycline: production, waste treatment and environmental impact assessment, *Braz. J. Pharm. Sci.*, 50 (2014) 25–40.
- [2] S. Pyörälä, K.E. Baptiste, B. Catry, E. Duijkeren, C. Greko, M.A. Moreno, M.C.M.F. Pomba, M. Rantala, M. Ružauskas, P. Sanders, E.J. Threlfall, J. Torren-Edo, K. Törnekem, Macrolides and lincosamides in cattle and pigs: use and development of antimicrobial resistance, *Vet. J.*, 200 (2014) 230–239.
- [3] R. Daghrir, P. Drogui, Tetracycline antibiotics in the environment: a review, *Environ. Chem. Lett.*, 11 (2013) 209–227.
- [4] S. Kim, P. Eichhorn, J.N. Jensen, A.S. Weber, D.S. Aga, Removal of antibiotics in wastewater: Effect of hydraulic and solid retention times on the fate of tetracycline in the activated sludge process, *Environ. Sci. Technol.*, 39 (2005) 5816–5823.
- [5] J.G. da Silva, M.A. Hyppolito, J.A. de Oliveira, A.P. Corrado, I.Y. Ito, I. Carvalho, Aminoglycoside antibiotic derivatives: Preparation and evaluation of toxicity on cochlea and vestibular tissues and antimicrobial activity, *Bioorg. Med. Chem.*, 15 (2007) 3624–3634.
- [6] C. Kowalski, M. Pomorska, B. Lebkowska, T. Slawik, Determination of oxytetracycline in biological matrix, *Acta Pol. Pharm.*, 63 (2006) 409–411.
- [7] J. Rivera-Utrilla, M. Sánchez-Polo, M.Á. Ferro-García, G. Prados-Joya, R. Ocampo-Pérez, Pharmaceuticals as emerging contaminants and their removal from water. A review, *Chemosphere*, 93 (2013) 1268–1287.
- [8] F. Trotta, C. Baggiani, M.P. Luda, E. Drioli, T. Massari, A molecular imprinted membrane for molecular discrimination of tetracycline hydrochloride, *J. Membr. Sci.*, 254 (2005) 13–19.
- [9] J. Rivera-Utrilla, C.V. Gómez-Pacheco, M. Sánchez-Polo, J.J. López-Peñalver, R. Ocampo-Pérez, Tetracycline removal from water by adsorption/bioadsorption on activated carbons and sludge-derived adsorbents, *J. Environ. Manage.*, 131 (2013) 16–24.
- [10] Y. Liu, H. Liu, Z. Zhou, T. Wang, C.N. Ong, C.D. Vecitis, Degradation of the common aqueous antibiotic tetracycline using a carbon nano tube electrochemical filter, *Environ. Sci. Technol.*, 49 (2015) 7974–7980.
- [11] C. Reyes, J. Fernández, J. Freer, M.A. Mondaca, C. Zaror, S. Malato, H.D. Mansilla, Degradation and inactivation of tetracycline by TiO<sub>2</sub> photocatalysis, *J. Photochem. Photobiol. A*, 184 (2006) 141–146.
- [12] Q. Zhou, M. Wang, A. Li, C. Shuang, M. Zhang, X. Liu, L. Wu, Preparation of a novel anion exchange group modified hyper-cross linked resin for the effective adsorption of both tetracycline and humic acid, *Front. Environ. Sci. Eng.*, 7 (2013) 412–419.
- [13] R. Hao, X. Xiao, X. Zuo, J. Nan, W. Zhang, Efficient adsorption and visible-light photocatalytic degradation of tetracycline hydrochloride using mesoporous BiOI microspheres, *J. Hazard. Mater.*, 209–210 (2012) 137–145.
- [14] M. Rathod, S. Haldar, S. Basha, Nano crystalline cellulose for removal of tetracycline hydrochloride from water via biosorption: Equilibrium, kinetic and thermodynamic studies, *Ecol. Eng.*, 84 (2015) 240–249.
- [15] M. Ersan, U.A. Guler, U. Acikel, M. Sarioglu, Synthesis of hydroxyapatite/clay and hydroxyapatite/pumice composites for tetracycline removal from aqueous solutions, *Process Saf. Environ. Protect.*, 96 (2015) 22–32.
- [16] Z. Zhang, H. Liu, L. Wu, H. Lan, J. Qu, Preparation of amino-Fe(III) functionalized mesoporous silica for synergistic adsorption of tetracycline and copper, *Chemosphere*, 138 (2015) 625–632.
- [17] W.C. Li, M.H. Wong, A comparative study on tetracycline sorption by *Pachydietyon coriaceum*, and *Sargassum hemiphylum*, *Int. J. Environ. Sci. Technol.*, 12 (2015) 2731–2740.
- [18] L. Zhang, X. Song, X. Liu, L. Yang, F. Pan, J. Lv, Studies on the removal of tetracycline by multi-walled carbon nanotubes, *Chem. Eng. J.*, 178 (2011) 26–33.
- [19] H. Chen, H. Luo, Y. Lan, T. Dong, B. Hu, Y. Wang, Removal of tetracycline from aqueous solutions using polyvinylpyrrolidone (PVP-K30) modified nanoscale zero valent iron, *J. Hazard. Mater.*, 192 (2011) 44–53.
- [20] Y. Chao, W. Zhu, X. Wu, F. Hou, S. Xun, P. Wu, H. Ji, H. Xu, H. Li, Application of graphene-like layered molybdenum disulfide and its excellent adsorption behavior for doxycycline antibiotic, *Chem. Eng. J.*, 243 (2014) 60–67.
- [21] Y. Chao, W. Zhu, J. Chen, P. Wu, X. Wu, H. Li, C. Han, S. Yan, Development of novel graphene-like layered hexagonal boron nitride for adsorptive removal of antibiotic gatifloxacin from aqueous solution, *Green Chem. Lett. Rev.*, 7 (2014) 330–336.
- [22] K.S. Novoselov, A.K. Geim, S.V. Morozov, D. Jiang, Y. Zhang, S.V. Dubonos, I.V. Grigorieva, A.A. Firsov, Electric field effect in atomically thin carbon films, *Science*, 306 (2004) 666–669.
- [23] C.N.R. Rao, A.K. Sood, K.S. Subrahmanyam, A. Govindaraj, Graphene: the new two-dimensional nanomaterial, *Angew Chem. Int. Ed.*, 48 (2009) 7752–7777.
- [24] J. Lakshmi, S. Vasudevan, Graphene—a promising material for removal of perchlorate (ClO<sub>4</sub><sup>-</sup>) from water, *Environ. Sci. Pollut. Res.*, 20 (2013) 5114–5124.
- [25] J. Lee, K.A. Min, S. Hong, G. Kim, Ab initio study of adsorption properties of hazardous organic molecules on graphene: Phenol, phenyl azide, and phenylnitrene, *Chem. Phys. Lett.*, 618 (2015) 57–62.
- [26] J. Xu, L. Wang, Y. Zhu, Decontamination of bisphenol A from aqueous solution by graphene adsorption, *Langmuir*, 28 (2012) 8418–8425.
- [27] S.M. Maliyekkal, T.S. Sreepasad, D. Krishnan, S. Kouser, A.K. Mishra, U.V. Waghmare, T. Pradeep, Graphene: a reusable substrate for unprecedented adsorption of pesticides, *Small*, 9 (2013) 273–283.
- [28] G.K. Ramesh, A.V. Kumara, H.B. Muralidhara, S. Sampath, Graphene and graphene oxide as effective adsorbents toward anionic and cationic dyes, *Colloid Interface Sci.*, 361 (2011) 270–277.
- [29] P. Ganesan, R. Kamaraj, S. Vasudevan, Application of isotherm, kinetic and thermodynamic models for the adsorption of nitrate ions on graphene from aqueous solution, *J. Taiwan Inst. Chem. Eng.*, 44 (2013) 808–814.

- [30] R. Kamaraj, A. Pandiarajan, M.R. Gandhi, A. Shibayama, S. Vasudevan, Eco-friendly and easily prepared graphene nano sheets for safe drinking water: Removal of chlorophenoxyacetic acid herbicides, *Chemistry Select*, 2 (2017) 342–355.
- [31] M.R. Gandhi, S. Vasudevan, A. Shibayama, M. Yamada, Graphene and graphene-based composites: A rising star in water purification - A comprehensive overview *Chemistry Select*, 1 (2016) 4358–4385.
- [32] S. Vasudevan, J. Lakshmi, The adsorption of phosphate by graphene from aqueous solution, *Rsc Adv.*, 2 (2012) 5234–5242.
- [33] X. Zhang, Y. Feng, S. Tang, W. Feng, Preparation of a graphene oxide-phthalocyanine hybrid through strong  $\pi$ - $\pi$  interactions, *Carbon*, 48 (2010) 211–216.
- [34] H. Guo, T. Jiao, Q. Zhang, W. Guo, Q. Peng, X. Yan, Preparation of graphene oxide-based hydrogels as efficient dye adsorbents for wastewater treatment, *Nano scale Res. Lett.*, 10 (2015) 1–10.
- [35] E.E. Ghadim, F. Manouchehri, G. Soleimani, H. Hosseini, S. Kimiagar, S. Nafisi, Adsorption properties of tetracycline onto graphene oxide: equilibrium, kinetic and thermodynamic studies, *Plos One*, 8 (2013) e79254.
- [36] Y. Gao, Y. Li, L. Zhang, H. Huang, J. Hu, S.M. Shah, X. Su, Adsorption and removal of tetracycline antibiotics from aqueous solution by graphene oxide, *J. Colloid Interface Sci.*, 368 (2012) 540–546.
- [37] U. Saha, Colorimetric determination of tetracycline derivatives in pharmaceutical preparations, *J. AOAC*, 72 (1989) 242–244.
- [38] U. Saha, Colorimetric determination of tetracycline hydrochloride in pharmaceutical preparations, *J. AOAC*, 70 (1987) 686–688.
- [39] H.-T. Fan, J.-X. Liu, H. Yao, Z.-G. Zhang, F. Yan, W.-X. Li, Ionic imprinted silica-supported hybrid sorbent with an anchored chelating schiff base for selective removal of cadmium(II) ions from aqueous media, *Ind. Eng. Chem. Res.*, 53 (2014) 369–378.
- [40] Y. Zhao, X. Gu, S. Gao, J. Geng, X. Wang, Adsorption of tetracycline (TC) onto montmorillonite: Cations and humic acid effects, *Geoderma*, 183–184 (2012) 12–18.
- [41] L. Ji, W. Chen, J. Bi, S. Zheng, Z. Xu, D. Zhu, P.J. Alvarez, Adsorption of tetracycline on single-walled and multi-walled carbon nanotubes as affected by aqueous solution chemistry, *Environ. Toxicol. Chem.*, 29 (2010) 2713–2719.
- [42] D.H. Carrales-Alvarado, R. Ocampo-Pérez, R. Leyva-Ramos, J. Rivera-Utrilla, Removal of the antibiotic metronidazole by adsorption on various carbon materials from aqueous phase, *J. Colloid Interface Sci.*, 436 (2014) 276–285.
- [43] S. Lagergren, About the theory of so-called adsorption of soluble substances, *Kungliga Svenska Vetensk. Handl.*, 24 (1898) 1–39.
- [44] Y.S. Ho, G. McKay, Pseudo-second-order model for sorption processes, *Process Biochem.*, 34 (1999) 451–465.
- [45] W.J. Weber, J.C. Morris, Kinetics of adsorption of carbon from solutions, *J. Sanit. Eng. Div. Am. Soc. Civ. Eng.*, 89 (1963) 31–63.
- [46] R.O.A. Rahman, H.A. Ibrahim, M. Hanafy, N.M.A. Monem, Assessment of synthetic zeolite Na A-X as sorbing barrier for strontium in a radioactive disposal facility, *Chem. Eng. J.*, 157 (2010) 100–112.
- [47] H. Javadian, Application of kinetic, isotherm and thermodynamic models for the adsorption of Co(II) ions on polyaniline/polypyrrole copolymer nano fibers from aqueous solution, *J. Ind. Eng. Chem.*, 20 (2014) 4233–4241.
- [48] R. Kamaraj, A. Pandiarajan, S. Jayakiruba, M. Naushad, S. Vasudevan, Kinetics, thermodynamics and isotherm modeling for removal of nitrate from liquids by facile one-pot electrosynthesized nano zinc hydroxide, *J. Mol. Liq.*, 215 (2016) 204–211.
- [49] Y. Seki, K. Yurdakoç, Equilibrium, kinetics and thermodynamic aspects of promethazine hydrochloride sorption by iron rich smectite, *Colloids Surf. A*, 340 (2009) 143–148.
- [50] I. Langmuir, The adsorption of gases on plane surfaces of glass, mica and platinum, *J. Am. Chem. Soc.*, 40 (1918) 1361–1403.
- [51] H.M.F. Freundlich, Über die adsorption in lösungen, *Z. Phys. Chem.* 57 (1906) 385–470.
- [52] M.M. Dubinin, L.V. Radushkevich, Equation of the characteristic curve of activated charcoal, *Chem. Zentr.*, 1 (1947) 875.
- [53] H. Javadian, P. Vahedian, M. Toosi, Adsorption characteristics of Ni(II) from aqueous solution and industrial wastewater onto Polyaniline/HMS nanocomposite powder, *Appl. Surf. Sci.*, 284 (2013) 13–22.
- [54] S. Vasudevan, J. Lakshmi, Studies relating to an electrochemically assisted coagulation for the removal of chromium from water using zinc anode, *Water Sci. Technol. Water Suppl.*, 11 (2011) 142–150.
- [55] H.-T. Fan, Y. Sun, Q. Tang, W.-L. Li, T. Sun, Selective adsorption of antimony(III) from aqueous solution by ion-imprinted organic-inorganic hybrid sorbent: Kinetics, isotherms and thermodynamics, *J. Taiwan Inst. Chem. Eng.*, 45 (2014) 2640–2648.
- [56] R. Kamaraj, S. Vasudevan, Facile one-pot synthesis of nano-zinc hydroxide by electro-dissolution of zinc as a sacrificial anode and the application for adsorption of Th<sup>4+</sup>, U<sup>3+</sup>, and Ce<sup>4+</sup>, from aqueous solution, *Res. Chem. Intermed.*, 42 (2016) 4077–4095.
- [57] S. Vasudevan, J. Lakshmi, G. Sozhan, Simultaneous removal of Co, Cu, and Cr from water by electro coagulation *Toxicol. Environ. Chem.*, 94 (2012) 1930–1940.